

ОБЪЕДИНЕННЫЙ  
ИНСТИТУТ  
ЯДЕРНЫХ  
ИССЛЕДОВАНИЙ  
ДУБНА

B 58

E2-87-287

**S.I.Bilenkaya, D.B.Stamenov**

**NEXT-TO-LEADING ORDER QCD-ANALYSIS  
OF EMC DEEP INELASTIC  
 $\mu p$  AND  $\mu d$  SCATTERING DATA**

Submitted to "Nuclear Physics, B"

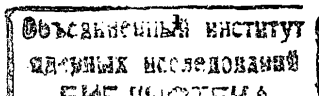
**1987**

## 1. Introduction

It seems today that quantum chromodynamics (QCD) is a very good candidate to be a theory of strong interactions. The QCD predictions are in good qualitative agreement with a great number of data on lepton-hadron and hadron-hadron processes in a large kinematic region. That is why a detailed quantitative verification of QCD is of great interest. The QCD-analysis of the data on deep inelastic lepton-nucleon scattering is one of the best ways to do that. To test the weak  $Q^2$  dependence of the nucleon structure functions as predicted by QCD, high statistics data for a large  $Q^2$  range are needed. This is just the case of deep inelastic lepton-nucleus scattering experiments. However, if we want to check also the quark-parton ideas on the nucleon structure these experiments cannot be used now to determine the parton distributions in the free nucleon. This is due to the discovery /1/ of an anomaly in the ratio of the structure function  $F_2$  measured on heavy nucleus to the structure function  $F_2^{D_2}$  measured on deuterium (the so-called EMC effect). This effect has confirmed again the important role of the deep inelastic lepton scattering off hydrogen and deuterium targets for the nucleon structure study.

The aim of this paper is a next-to-leading order (NLO) QCD-analysis of the EMC data on deep inelastic  $\mu p$  /2/ and  $\mu d$  /3/ scattering experiments. Due to high statistics, one of the main advantages of these experiments is an accurate measurement of the  $Q^2$  dependence of the free and quasifree nucleon structure functions in a large kinematic range.

There are two reasons to involve next-to-leading order QCD corrections to the structure functions. First of all, the QCD scale parameter  $\Lambda$  determined by the experimental data can be connected



with the used renormalization scheme in unique way only if these corrections are taken into account /4/. Secondly, having in mind the available  $Q^2$  values at present, these corrections are not negligible in the high  $x$  range.

In contrast to the majority of papers on this subject the cross section data on deep inelastic scattering (not the experimental values for the nucleon structure functions obtained from these data by additional extrapolations and assumptions) are analysed. The nucleon structure functions  $F_2$  and  $F_L$  (or  $R$ ) are given in terms of parton distributions. The expressions for these functions predicted by QCD in the desired approximation are substituted in the cross section formula for deep inelastic muon scattering off nucleons (eq.(1) below). Then, the theoretical cross sections thus obtained are compared with their experimental values. The QCD parameter and all parameters associated with the parametrisation of the parton distributions are determined by fitting the cross section data. In such an approach, firstly, additional extrapolations which decrease the precision of the measured cross sections are not needed, and secondly, the complete set of experimental data on cross sections is used. For that reason we consider that such a test of the QCD predictions for the deep inelastic lepton-nucleon processes has definite advantages today.

## 2. Method of Analysis

The method of analysis was described in detail in our previous papers /5,6/. In these papers, a leading order QCD fit to the data on deep inelastic muon-nucleon scattering has been done. Here, we are going to recall only the basic features of the method and to give some necessary formulae taking into account the next-to-leading order corrections to the nucleon structure functions.

The measured differential cross section for the deep inelastic muon-nucleon scattering in one photon exchange approximation takes the following form in the EMC kinematic region

$$\frac{d^2\sigma}{dx dQ^2} = \frac{4\pi\alpha^2}{xQ^4} \left[ \left(1 - \gamma + \frac{\gamma^2}{2}\right) F_2(x, Q^2) - \frac{\gamma^2}{2} F_L(x, Q^2) \right], \quad (1)$$

where  $Q^2$  is the momentum transfer squared,  $x = Q^2/2M\nu$  is the Bjorken scaling variable,  $\gamma = \nu/E$ ,  $\nu = E - E'$ ,  $E$  and  $E'$  are the muon initial and final energy, respectively. In eq.(1)  $F_2$  and  $F_L$  are the nucleon structure functions depending on  $x$  and  $Q^2$ . The longitudinal structure function  $F_L$  is defined as

$$F_L(x, Q^2) = F_2(x, Q^2) - 2x F_1(x, Q^2). \quad (2)$$

In leading order (LO) QCD, the Callan-Gross relation /7/ between  $F_1$  and  $F_2$

$$2x F_1^{LO}(x, Q^2) = F_2^{LO}(x, Q^2) \quad (3)$$

is true and in this approximation

$$F_L^{LO}(x, Q^2) = 0. \quad (4)$$

The cross section (1) is usually written in terms of  $F_2$  and the ratio

$$R \equiv \frac{\sigma_L}{\sigma_T} = \frac{(1 + 4M^2x^2/Q^2) F_2 - 2x F_1}{2x F_1}, \quad (5)$$

where  $\sigma_L$  and  $\sigma_T$  are the longitudinal and transverse total photoabsorption cross sections.

In leading order QCD approximation the quantity  $R$  is also equal to zero:

$$R^{LO}(x, Q^2) = 0 \quad (6)$$

and then there is one-to-one correspondence between the measured cross section (1) and the structure function  $F_2^{LO}$ . In this case, analysis based on the fit of  $F_2$  to the cross section data or to the extracted from these data values for  $F_2$  assuming  $R = 0$  are equivalent.

However, in the next-to-leading order QCD approximation  $F_L$  is different from zero and has the form

$$F_L^{NLO}(x, Q^2) = \frac{\alpha^{LO}(Q^2)}{4\pi} x^2 \int_x^1 \frac{dy}{y^3} \left[ \frac{16}{3} F_2^{LO}(y, Q^2) + \frac{20}{9} N_f (1 - \frac{x}{y}) \gamma G^{LO}(y, Q^2) \right]. \quad (7)$$

Here  $N_f$  is the number of flavour,  $F_2^{LO}(x, Q^2)$  and  $G^{LO}(x, Q^2)$  are the leading order expressions for  $F_2$  and the gluon distribution in the free nucleon.

There are two ways to test the next-to-leading order corrections to  $F_L$  and  $F_2$ . In the first one, the theoretical predictions for  $F_L$  and  $F_2$  are compared with the model-independent experimental values of these quantities. In the second, the theoretical cross sections (1) accounting the next-to-leading order corrections to  $F_L$  (eq. (7)) and  $F_2$  (eqs. (8a,b)) below are fitted to the directly measured values of these cross sections.

The determination of  $F_2$  and  $F_L$  (instead of  $\frac{F_L}{F_2}$  the ratio  $R$  is usually determined by the experimentalists) in a model-independent way is a difficult experimental task: Cross section data at fixed  $x$  and  $Q^2$  but at different values of muon beam energy are needed. The application of such a procedure for the available data requires additional extrapolations. As a result, the accuracy in determination of  $R$  is much smaller than that of the measured cross sections. Moreover, it is impossible to use completely the information on the cross section data in this procedure. For instance, the data points  $(x, Q^2)$  at one or two values of the beam energy are not used for determination of  $R$ . For that reason the  $(x, Q^2)$  region,

where  $R(F_L)$  and  $F_2$  are model-independently determined is smaller than that of the cross section data. That is why we consider that a direct QCD-analysis of the cross section data on deep inelastic muon-nucleon scattering has advantages at present.

Before continuing the description of our method of analysis let us mention also two QCD fits to the data which can be found in the literature and seem to be inconsistent. In the first one, the values for  $F_2$  obtained from the cross section data by assumption that  $R = 0$  are compared with the next-to-leading order prediction for  $F_2$ :  $F_2^{NLO}(x, Q^2)$ . But in this approximation of QCD  $R$  is different from zero:  $R^{NLO}(x, Q^2) \neq 0$ ! In the second test, the values for  $F_2$  found from the cross section data by assuming  $R = R^{NLO}$  are fitted by the leading order expression for the structure function  $F_2$ :  $F_2^{LO}(x, Q^2)$ . We think that such a test is inconsistent too.

In the next-to-leading order QCD the proton and deuteron structure functions  $F_2^{(p)}$  and  $F_2^{(d)}$  can be represented as

$$F_2^{(p)NLO}(x, Q^2) = \frac{4}{9} x u_v^{NLO}(x, Q^2) + \frac{1}{9} x d_v^{NLO}(x, Q^2) + \frac{2}{9} x S^{NLO}(x, Q^2) + \frac{4}{9} x C^{NLO}(x, Q^2), \quad (8a)$$

$$\frac{1}{2} F_2^{(d)NLO}(x, Q^2) = \frac{5}{18} (x u_v^{NLO}(x, Q^2) + x d_v^{NLO}(x, Q^2)) + \frac{2}{9} x S^{NLO}(x, Q^2) + \frac{4}{9} x C^{NLO}(x, Q^2), \quad (8b)$$

where

$$S = 6s, \quad C = 2c \quad (\bar{c} = c).$$

In eqs. (8a,b)  $u_v, d_v, S$  and  $c$  are the valence  $u$  and  $d$ , strange and charm quark distributions in the free proton. It should be noted that the SU(3)-symmetry of the sea quark distributions and eq.  $\bar{c} = c$  are assumed in order to obtain these expressions for  $F_2$ . In eq. (8b) the assumption that the deuteron is a system of two quasifree nucleons is also made. Note, however, that unless the origin of the EMC effect /1/ is cleared this conjecture will remain questionable.

It is known /8,9/ that definition of the parton distributions beyond the leading order is not unique. In eqs. (8a,b) the definition /9/ in which the parton formulae for  $F_2$  hold is used. Note also that the parton distributions in this definition are renormalization-prescription independent.

The quark distributions in eqs. (8a,b) satisfy the Lipatov-Altarelli-Parisi (LAP) equations /10/ in the next-to-leading order QCD or the corresponding evolution equations for the moments of these distributions (s.g. ref. (4)). There are several methods to solve these equations approximately. In this paper the method suggested by Buras and Gaemers /11/ is used. According to this method, the following parametrisations for the parton distributions are assumed:

$$x u_v^{NLO}(x, Q^2) = \Gamma_u(\tilde{s}) x^{\eta_1(\tilde{s})} (1-x)^{\eta_2(\tilde{s})}, \quad (9a)$$

$$x d_v^{NLO}(x, Q^2) = \Gamma_d(\tilde{s}) x^{\eta_3(\tilde{s})} (1-x)^{\eta_4(\tilde{s})}, \quad (9b)$$

$$x S^{NLO}(x, Q^2) = A_s(\tilde{s}) (1-x)^{\eta_5(\tilde{s})}, \quad (9c)$$

$$x C^{NLO}(x, Q^2) = A_c(\tilde{s}) (1-x)^{\eta_c(\tilde{s})}, \quad (9d)$$

$$x G^{LO}(x, Q^2) = A_g(\tilde{s}) (1-x)^{\eta_g(\tilde{s})}, \quad (10)$$

which are a simple generalization of these distributions at  $Q^2 = Q_0^2$ .

In eqs. (9a-d)

$$\tilde{s} = \ln \left[ \frac{\alpha^{NLO}(Q_0^2)}{\alpha^{NLO}(Q^2)} \right], \quad (11)$$

where  $\alpha^{NLO}(Q^2)$  is the next-to-leading order running coupling constant of strong interactions

$$\alpha^{NLO}(Q^2) = \frac{4\pi}{\beta_0 \ln(Q^2/\Lambda^2)} \left[ 1 - \frac{\beta_1}{\beta_0} \frac{\ln \ln(Q^2/\Lambda^2)}{\ln(Q^2/\Lambda^2)} \right] \quad (12)$$

$$\text{with } \beta_0 = 11 - \frac{2}{3} N_f, \quad \beta_1 = 102 - \frac{38}{3} N_f. \quad (13)$$

The coefficients  $\Gamma_u(\tilde{s})$  and  $\Gamma_d(\tilde{s})$  in eqs. (9a,b) are determined by the parton sum rules

$$\int_0^1 u_v(x, Q^2) dx = 2, \quad \int_0^1 d_v(x, Q^2) dx = 1 \quad (14)$$

and in our case they take the form

$$\Gamma_u(\tilde{s}) = 2 \frac{\Gamma(\eta_1(\tilde{s}) + \eta_2(\tilde{s}) + 1)}{\Gamma(\eta_1(\tilde{s})) \Gamma(\eta_2(\tilde{s}) + 1)}, \quad (15a)$$

$$\Gamma_d(\tilde{s}) = \frac{\Gamma(\eta_3(\tilde{s}) + \eta_4(\tilde{s}) + 1)}{\Gamma(\eta_3(\tilde{s})) \Gamma(\eta_4(\tilde{s}) + 1)}. \quad (15b)$$

In eqs. (15a,b)  $\Gamma$  is Euler's gamma function.

Note that in eq. (10)  $\tilde{s}$  is given by the ratio of the leading order strong coupling constants

$$\tilde{s} = \ln \left( \frac{\alpha^{LO}(Q_0^2)}{\alpha^{LO}(Q^2)} \right), \quad (16)$$

where

$$\alpha^{LO}(Q^2) = \frac{4\pi}{\beta_0 \ln(Q^2/\Lambda_{LO}^2)}. \quad (17)$$

For the leading order quark distributions, involved in  $F_L^{NLO}(x, Q^2)$  via the structure function  $F_2^{LO}(x, Q^2)$ , parametrisations of the kind (9a-d) (replacing  $\tilde{s}$  by  $\bar{s}$ ) are used.

The exponents  $\eta_i(\xi)$  in eqs. (9a,b) are taken to be linear functions of  $\xi$

$$\eta_i(\xi) = \eta_i(0) + \eta_i' \xi, \quad i=1, \dots, 4. \quad (18)$$

The slopes  $\eta_i'$  are determined from the requirement that the valence quark distributions (9a,b) have to reproduce the next-to-leading order QCD predictions for their first 20 moments with an accuracy not smaller than 1-1.5%. It turns out that this condition can be fulfilled for the EMC kinematic range. As has been already shown /12/, this accuracy of the moment approximation is enough to reproduce correctly the numerical solutions of the LAP equations for the valence distributions in the range  $0.02 < x < 0.80$ .

The quantities

$$\eta_i \equiv \eta_i(0), \quad A_s \equiv A_s(0), \quad \eta_s \equiv \eta_s(0), \quad \eta_G \equiv \eta_G(0) \quad (19)$$

(the assumption  $A_c(0) = 0$  is used) are free parameters associated with the parton distributions at some fixed value of  $Q^2 = Q_0^2$  from the kinematic range of the experiments. It is convenient, in practice, to choose  $Q_0^2 = Q_{\min}^2$ . There are experimental

evidences /13/ that the sea quark distributions are close to zero in the range  $x > 0.35$ . Then, the quantities  $A_s(\xi)$ ,  $\eta_s(\xi)$

$A_c(\xi)$  and  $\eta_c(\xi)$  can be written explicitly /11/ as functions of the parameters (19) and  $\Lambda$  using only the first two QCD moments. In the paper /11/ this has been done in the leading order QCD. However, it is a simple task to repeat this procedure taking into account the next in  $\alpha_s$  corrections.

In contrast with refs. /11,12/ the values of the parameters

$\{\Lambda_{\text{QCD}}; \eta_i, A_s, \eta_s; \eta_i'\}$  are determined by a simultaneous fit to the cross section data and the next-to-leading

order QCD equations for the moments of the valence quark distributions. All numerical values of the quantities involved in these equations are taken in correspondence of the so-called  $\overline{\text{MS}}$  renormalization scheme /14,15/.

Ending this section we would like to note that any one than the Buras-Gasmer method could be used to solve the QCD equations for the parton distributions. We have applied it because of the simple analytic parametrisations of these distributions which are convenient and useful for practical purposes. Besides, these parametrisations approximate the exact solutions of QCD equations with an accuracy better enough than the precision of the available at present data.

### 3. Results of the Analysis

In this section we give the results of our simultaneous fit to the EMC deep inelastic  $\mu p$  /2/ and  $\mu d$  /3/ scattering data in the following kinematic region:

$$\begin{aligned} \mu p: & \quad 0.02 < x < 0.80, \quad 5 < Q^2 < 170 \text{ GeV}^2; \\ \mu d: & \quad 0.02 < x < 0.80, \quad 7 < Q^2 < 170 \text{ GeV}^2. \end{aligned}$$

We have chosen  $Q_0^2 = 5 \text{ GeV}^2$ . However, the values of  $\Lambda_{\overline{\text{MS}}}$  and  $\chi^2/\text{DOF}$  were not sensitive to this particular choice of  $Q_0^2$ . It is well known that the shape of the gluon distribution and  $\Lambda$  are strongly correlated. The influence of the power  $\eta_G$  on  $\Lambda$  has been discussed in detail in our previous paper /5/. Here we have fixed  $\eta_G = 5$ . This value of  $\eta_G$  is in agreement with the results of the EMC analysis /2/. In all fits only statistical errors are taken into account. Free normalization factors  $N_i$  and  $N_d$  are introduced to account for the relative normalisation between data sets at different incident energies and different targets.

'Higher twist' corrections to the nucleon structure functions are not included in this analysis. As has been shown in ref. /2/, their contribution to the structure functions can be neglected in the EMC kinematic region.

The results of analysis are presented in tables 1 and 2. Let us start our discussion with the non-singlet fit results in the range  $x > 0.3$ . As has been already noted, there are strong evidences from the neutrino scattering experiments that the sea quark distributions are close to zero in this region. Then, the gluon distribution

$G(x, Q^2)$  can be neglected too and the QCD-fit to the data in that region is independent of the assumption on the shape of gluons. So, in this case the proton and deuteron structure functions are expressed only via the valence quark distributions. The value of  $\Lambda_{\overline{MS}}$  as determined by the next-to-leading order fit is

$$\Lambda_{\overline{MS}} = 218 \pm 73 \text{ MeV}.$$

The obtained values for the exponents  $\eta_i$  (see table 2) are close to those based on the quark counting rules and Regge-pole mechanism. The corresponding value of  $\chi^2/\text{DOF}$  is

$$\chi^2/\text{DOF} = 177/136$$

and the EMC data for the range  $0.3 < x < 0.8$  are described by this non-singlet fit on 1.1% confidence level.

The mean value of  $\Lambda_{\overline{MS}}$  is different from that obtained by the EMC analysis /2/:

$$\Lambda_{\overline{MS}} = 105^{+55}_{-45},$$

but in one standard deviation these values are in agreement. Note that unlike ref. /2/, where only the  $\mu p$  scattering data were analysed, we have involved also to the fit the data on muon-deuteron scattering. We want to mention also the following property of our

Table 1  
The results of QCD fits to the EMC cross section data  
on deep inelastic  $\mu p$  and  $\mu d$  scattering

$x > 0.3$ (145 exp. points)	$0.07 < x < 0.80$ (260 exp. points)	$0.02 < x < 0.80$ (285 exp. points)
$\Lambda_{\overline{MS}}$ (MeV)	$\Lambda_{\overline{MS}}$ (MeV)	$\Lambda_{\overline{MS}}$ (MeV)
$\chi^2/\text{DOF}$	$\chi^2/\text{DOF}$	$\chi^2/\text{DOF}$
L0	223 ± 65	80 ± 19
	176/136	409/272
MLO	218 ± 73	68 ± 20
	177/136	384/245
	65 ± 20	454/266

Table 2

The values of the free parameters as determined by our QCD fits to the EMC

$\mu p$  and  $\mu d$  scattering data ( $N_f=4$ ,  $\gamma_e=5$ ,  $N_1(E=120 \text{ GeV})=1$ )

	$\gamma_1$	$\gamma_2$	$\gamma_3$	$\gamma_4$	$\gamma_5$	$A_5$	$\gamma_5$	$N_2$	$N_3$	$N_4$
	$\gamma_1$	$\gamma_2$	$\gamma_3$	$\gamma_4$	$\gamma_5$	$A_5$	$\gamma_5$	$E=200 \text{ GeV}$	$E=240 \text{ GeV}$	$E=280 \text{ GeV}$
LO	0.62±0.04	2.79±0.09	0.91±0.18	4.83±0.87	—	—	—	1.07±0.02	1.08±0.02	1.04±0.02
	-0.19±0.01	0.75±0.02	-0.30±0.06	0.77±0.05	—	—	—	—	—	—
NLO	0.61±0.04	2.72±0.12	0.88±0.18	5.32±1.53	—	—	—	1.07±0.02	1.08±0.02	1.04±0.02
	-0.14±0.02	1.18±0.04	-0.27±0.07	1.34±0.11	—	—	—	—	—	—
NLO	0.63±0.01	2.88±0.05	0.72±0.08	4.65±0.31	2.04±0.25	26.1±3.1	0.97±0.01	0.98±0.01	0.97±0.01	0.97±0.01
	-0.18±0.02	1.01±0.03	-0.23±0.03	1.13±0.04	—	—	—	—	—	—
LO	0.64±0.01	2.89±0.04	0.86±0.05	5.03±0.28	1.22±0.05	18.3±1.0	0.97±0.01	0.99±0.01	0.98±0.01	0.98±0.01
	-0.19±0.01	0.78±0.02	-0.29±0.02	0.79±0.03	—	—	—	—	—	—
NLO	0.62±0.01	2.85±0.05	0.70±0.06	4.49±0.32	1.64±0.12	20.1±1.8	0.97±0.01	0.98±0.01	0.98±0.01	0.98±0.01
	-0.17±0.02	1.03±0.03	-0.22±0.03	1.14±0.04	—	—	—	—	—	—

fit to the data for the range  $x > 0.3$ . In this range the structure function  $F_2^{(p)th}(x, Q^2)$  has the form

$$F_2^{(p)th}(x, Q^2) = \frac{4}{9} x u_v(x, Q^2) + \frac{1}{9} x d_v^{NLO}(x, Q^2). \quad (20)$$

Taking into account the sum rules (14) for the valence distributions  $u_v$  and  $d_v$ , the structure function  $F_2^{(p)th}(x, Q^2)$  determined by this fit satisfies for any  $Q^2$  the following condition:

$$\int_0^1 \frac{dx}{x} F_2^{(p)th}(x, Q^2) = 1. \quad (21)$$

This is not true for the structure function  $F_2^{(p)th}(x, Q^2)$  which has been used in ref./2/.

The data for the whole  $x$  range were also analysed in the next-to-leading order QCD. At low  $x$  the sea cannot be neglected. To eliminate complications associated with the charm threshold at small  $x$  the range  $0.02 < x < 0.07$  has been excluded from the data analysis. Only the lowest  $Q^2$  points of this region were used to constrain the low  $x$  behaviour of quark and gluon distributions. As has been discussed above, for the shape of the gluon distribution the following assumption has been used:

$$x G(x, Q_0^2) = A_G (1-x)^5. \quad (22)$$

The coefficient  $A_G$  in (22) is fixed by the energy-momentum sum rule.

From the best fit to the data for the range  $0.07 < x < 0.80$  the following values for  $\Lambda_{\overline{MS}}$  and  $\chi^2/\text{DOF}$  are found:

$$\Lambda_{\overline{MS}} = 0.65 \pm 20 \text{ MeV}, \quad \chi^2/\text{DOF} = 384/245.$$

This mean value of  $\Lambda_{\overline{MS}}$  is approximately three times smaller than that determined by the next-to-leading order fit for the range  $x > 0.3$ . However, these values of  $\Lambda_{\overline{MS}}$  are in agreement in two standard error deviations. Note that the value of  $\chi^2/\text{DOF}$  remains



rather large (384/245) even if the experimental points introducing a large  $(\sum_{i=1}^n \Delta\chi_i^2 = 40)$  contribution to  $\chi^2$  are excluded. We would like to remark that the value of this quantity for the leading order fit in the whole  $x$  range given in ref./2/ is even larger. Note also that if the procedure suggested in ref. /16/ is performed and the statistical errors are multiplied by the scale factor

$$S = \sqrt{\chi^2/(n-1)}, \quad (23)$$

where  $n$  is the number of the experimental points the value of  $\chi^2/\text{DOF}$  becomes close to unity while the values of all free parameters remain practically unchanged.

In tables 1 and 2 the results of data analysis for the whole  $x$  range are presented too. The values of  $\Lambda_{\overline{MS}}$  and the other free parameters are practically the same. However, although eight data points with a very large contribution ( $\sum \Delta\chi_i^2 = 106$ ) in  $\chi^2$  have been omitted the value of  $\chi^2/\text{DOF}$  increases.

In tables 1 and 2 we give also the results of the leading order QCD analysis ( $F_L = 0$ ) of the EMC cross section data. The values of the parameters determined by this fit were used for the calculation of the longitudinal structure function  $F_L^{\text{NLO}}$  in the next-to-leading order (see eq.(7)).

#### 4. Summary

The EMC cross section data on deep inelastic  $\mu p$  and  $\mu d$  scattering have been analysed in the next-to-leading order QCD approximation. The free nucleon structure functions were expressed in terms of parton distributions. The Buras-Gaemers method was used to solve the QCD equations for these distributions. The values of  $\Lambda$  and all the free parameters connected with the parametrisation of the parton distributions have been determined from a simultaneous fit to

the cross section data and the next-to-leading order QCD equations for the moments of those distributions.

As usual, the analysis has been performed in the following regions:

i)  $x > 0.3$  where the contribution from the sea to the structure functions can be neglected (non-singlet fit) and

ii) whole  $x$  range where this contribution is important.

For  $\Lambda_{\overline{MS}}$  and  $\chi^2/\text{DOF}$  the following values were found:

$$x > 0.3: \Lambda_{\overline{MS}} = 218 \pm 73 \text{ MeV}, \chi^2/\text{DOF} = 177/136;$$

$$0.07 < x < 0.80: \Lambda_{\overline{MS}} = 65 \pm 20 \text{ MeV}, \chi^2/\text{DOF} = 384/245.$$

In the case  $x > 0.3$  the non-singlet parametrisation of  $F_2$  and  $F_L$  fits the data with 1.1% confidence level. In the whole  $x$  range, however, the data fit (as in the case of the leading order QCD) is not satisfactory. Let us emphasize (see table 1) that the data fit is not improved by involving the next-to-leading order QCD corrections to the structure functions. This fact is a common feature of most of the QCD-analyses given in the literature and probably it reflects the experimental situation now and the present QCD uncertainties.

Nevertheless, we consider that an approach according to which cross section data are used to test the QCD predictions for different deep inelastic lepton-nucleon processes has definite advantages today. In this connection, it is of interest to perform a combined analysis of the  $\mu(\nu)H_2$  and  $\mu(\nu)D_2$  cross section data. Despite much smaller statistics, the neutrino scattering data are more informative for the determination of the quark distributions in the free nucleon.

The authors are grateful to I.A.Savin for support and interest in this work. One of the authors (D.S.) is thankful to T.Sloan who has kindly supplied us with the EMC  $\mu D_2$  cross section data.

## References

- /1/ J.J.Aubert et al., Phys.Lett. 123B (1983) 275.
- /2/ J.J.Aubert et al., Nucl. Phys. B259 (1985) 189.
- /3/ J.J.Aubert et al., Phys.Lett. 123B (1983) 115.
- /4/ M.Bacé, Phys. Lett. 78B (1978) 132;  
A.J.Buras, Rev.Mod.Phys. 52 (1980) 199.
- /5/ S.I.Bilenkaya and D.B.Stamenov, Bulg. Journ. of Phys. 13 (1986) 485 and JINR preprint E2-85-380, Dubna (1985).
- /6/ S.I.Bilenkaya and D.B.Stamenov, JINR preprint P2-86-85, Dubna, (1986).
- /7/ C.G.Callan and D.J.Gross, Phys.Rev.Lett. 22 (1969) 156.
- /8/ L.Baulier and C.Kounnas, Nucl.Phys. B141 (1978) 423;  
J.Kodaira and T.Vematsu, Nucl.Phys. B141 (1978) 497.
- /9/ G.Altarelli, R.K.Ellis and G.Martinelli, Nucl.Phys. B143 (1978) 521; Nucl.Phys. B146 (1979) 544(E).
- /10/ L.N.Lipatov, Yad.Fiz. 20 (1974) 181;  
G.Altarelli and G.Parisi, Nucl.Phys. B126 (1977) 298.
- /11/ A.J.Buras, Nucl.Phys. B125 (1977) 125;  
A.J.Buras and K.J.F.Gaemers, Nucl.Phys. B132 (1978) 249.
- /12/ A.Bialas and A.J.Buras, Phys.Rev.D21 (1980) 1825.
- /13/ H.Abramowicz et al., Z.Phys. C17 (1983) 283;  
F.Bergsma et al., Phys.Lett.123B (1983) 269.
- /14/ E.G.Floratos, D.A.Ross and C.T.Sachrajda, Nucl.Phys. B129, (1977) 66 and Errata in Nucl.Phys. B139 (1978) 545; Nucl. Phys. B152 (1979) 493.
- /15/ W.A.Bardeen, A.J.Buras, D.W.Duke and T.Muta, Phys.Rev. D18 (1978) 3998.
- /16/ Reviews of Modern Phys., April 1984, vol.56. No2, part II.

Received by Publishing Department  
on April 24, 1987.

Биленькая С.И., Стаменов Д.Б.  
КХД анализ данных EMC по глубоконеупругому  $\mu p$ - и  $\mu d$ -рассеянию  
с учетом радиационных поправок

E2-87-287

Излагаются результаты совместного КХД анализа данных Европейской мюонной коллаборации (EMC) по глубоконеупругому  $\mu p$ - и  $\mu d$ -рассеянию с учетом радиационных поправок к структурным функциям нуклона. Эти функции выражаются через импульсные распределения партонов в нуклоне. Для решения КХД уравнений для партонных распределений используется метод Бураса-Гемерса. Поправки к структурным функциям от высших твистов не учитываются. Как было показано, их вклад несущественен в кинематической области EMC. В отличие от большинства работ анализ проводился по сечениям глубоконеупругого рассеяния (а не по полученным из них с помощью дополнительных экстраполяций и предположений значениям для структурных функций). Для параметра КХД  $\Lambda_{\overline{MS}}$  получены следующие значения: а)  $\Lambda_{\overline{MS}} = 218 \pm 73$  МэВ для несинглетного анализа данных в области  $x > 0,3$  и б)  $\Lambda_{\overline{MS}} = 65 \pm 20$  МэВ, если анализ данных проводился для всей кинематической области EMC.

Работа выполнена в Лаборатории теоретической физики ОИЯИ.

Препринт Объединенного института ядерных исследований. Дубна 1987

Bilenkaya S.I., Stamenov D.B.  
Next-to-Leading Order QCD-Analysis of EMC Deep Inelastic  
 $\mu p$  and  $\mu d$  Scattering Data

E2-87-287

A combined next-to-leading order QCD analysis of the European Muon Collaboration (EMC)  $\mu p$  and  $\mu d$  scattering data is presented. The nucleon structure functions are given in terms of parton distributions. The Buras-Gaemers method is used to solve the QCD equations for these distributions. The higher twist corrections are not taken into account. As has been shown their contribution to the structure functions is negligible. In the EMC kinematic region. Unlike most of the papers on this subject the cross section data (not the value for the structure functions obtained from these data by additional extrapolations and assumptions) are fitted. The following values for the QCD scale parameter  $\Lambda_{\overline{MS}}$  are found: i)  $\Lambda_{\overline{MS}} = 218 \pm 73$  MeV for the non-singlet fit to the data in the range  $x > 0.3$  and ii)  $\Lambda_{\overline{MS}} = 65 \pm 20$  MeV if the whole  $x$  data are fitted.

The investigation has been performed at the Laboratory of Theoretical Physics, JINR.

Preprint of the Joint Institute for Nuclear Research. Dubna 1987